A continuum determination of the strong isospin-breaking contribution to the muon anomalous magnetic moment

Kim Maltman[1,2⋆], Christopher James[3†] and Randy Lewis[3‡]

1 Department of Mathematics and Statistics, York University, 4700 Keele St., Toronto, Ontario, Canada M3J 1P3
2 CSSM, Department of Physics, University of Adelaide, Adelaide, SA 5005 Australia
3 Department of Physics and Astronomy, York University, 4700 Keele St., Toronto, Ontario, Canada M3J 1P3

⋆ kmaltman@yorku.ca , † cljames195@gmail.com , ‡ randy.lewis@yorku.ca

16th International Workshop on Tau Lepton Physics (TAU2021)
Online, September 27 - October 1, 2021
doi:10.21468/SciPostPhysProc.16

Abstract

First-principles lattice determinations of the Standard Model expectation for the leading order hadronic vacuum polarization contribution to the anomalous magnetic moment of the muon have become sufficiently precise that further improvement requires including strong and electromagnetic isospin-breaking effects. We provide a continuum estimate of the strong isospin-breaking contribution, $a_\mu^{\rm SIB}$, using $SU(3)$ chiral perturbation theory. The result is shown to be dominated by resonance-region contributions encoded in a single low-energy constant whose value is known from flavor-breaking hadronic τ decay sum rules. Implications of the form of the result for lattice determinations of $a_\mu^{\rm SIB}$ are also discussed.

Received 2021-12-10
Accepted 2024-12-18
Published 2025-07-15
doi:10.21468/SciPostPhysProc.16.031

Check for updates

Contents

1 Introduction

The more than 3 σ disagreement between the final 2006 BNL E821 result for a_μ [1–3], the anomalous magnetic moment of the muon, and subsequent updates of the Standard Model (SM) expectation prompted intense interest in improving both experimental and theoretical results. Interest in the latter has been further heightened by the recently released Fermilab E989 result [4], which produces an updated experimental world average 4.2σ higher than the current best assessment of the SM expectation [5].[1]

Hadronic contributions, though representing a small fraction of a_μ, dominate the uncertainty in the SM prediction. This paper focuses on the largest of these, the leading-order, hadronic vacuum polarization contribution, $a_\mu^{\rm LO,HVP}$.

As is well known, assuming (as expected) beyond-the-SM contributions to experimentally measured $e^+e^- \to hadrons$ cross sections are numerically negligible, the SM expectation for $a_\mu^{\rm LO,HVP}$ can be obtained as a weighted ("dispersive") integral over the inclusive hadroproduction cross-section ratio $R(s)$. The weight entering this integral is exactly known, monotonically decreasing with hadronic invariant squared mass, s, and strongly emphasizes contributions from the low-s region, with $\sim$ 73% of the full dispersive result coming from the $\pi\pi$ exclusive mode. Ref. [5] provides a detailed discussion of the most recent dispersive evaluations [11–13, 26].

A practical complication limiting the accuracy of these determinations is the long-standing discrepancy between BaBar [27,28] and KLOE [29] $e^+e^- \to \pi^+\pi^-$ cross section results, which independent determinations by CMD2 [30–32], BESIII [33], CLEO-c [34] and SND [35] have so far failed to resolve. The difference, 9.8×10^{-10} [13], between results for the $\pi\pi$ contribution obtained using only BaBar or KLOE in the region $0.305\ GeV < E_{CM} < 1.937\ GeV$, and the analogous difference, 5.5×10^{-10}, between the full $\pi\pi$ contribution obtained using averages with either BaBar or KLOE excluded [12], both considerably exceed the uncertainty anticipated from the full Fermilab E989 experimental program.

The reliance on at-present-discrepant experimental spectral data can, in principle, be avoided using lattice results for the electromagnetic (EM) current two-point function to evaluate $a_\mu^{\rm LO,HVP}$. This possibility was first raised in Ref. [36] and relies on the alternate representation of $a_\mu^{\rm LO,HVP}$ as a weighted integral of the subtracted EM vacuum polarization, $\hat\Pi_{EM}(Q^2) \equiv \Pi_{EM}(Q^2) - \Pi_{EM}(0)$ over spacelike $Q^2 = -s > 0$ [37, 38]. While the precision of the lattice determination has yet to reach that of the dispersive results, there has been rapid progress over the last few years, with recent updates from the BMW [39, 40], ETMC [41–43], RBC/UKQCD [44–46], FNAL/HPQCD/MILC [47, 48], Mainz [49], PACS [50] and Aubin *et al.* [51] collaborations. The most recent BMW result [40], in particular, reaches a precision of 0.8%. While (as detailed, e.g., in Ref. [46]) some disagreements persist between results from different lattice groups for the dominant ud connected contribution, as well as for the $t_0 = 0.4$ fm, $t_1 = 1.0$ fm, $\Delta = 0.15$ fm RBC/UKQCD "window" quantity $a_\mu^{ud,conn.,isospin,W}$ [44], these disagreements are the subject of ongoing scrutiny, and additional sub-%-level lattice results are expected in the near future from a number of other lattice groups.

The current sub-% precision goal for determining $a_\mu^{\rm LO,HVP}$ on the lattice necessitates an evaluation of the effects of strong and EM isospin-breaking (IB). These receive contributions from both quark-line-connected and -disconnected diagrams, with the latter much more numerically challenging on the lattice.

[1] The SM expectation assessment of Ref. [5] is based on the results of Refs. [6, 7] for the QED contribution, Refs. [8,9] for the electroweak contribution, Refs. [10–16] for hadronic vacuum polarization contributions through next-to-next-to-leading order, and Refs. [17–25] for the hadronic light-by-light contribution.

Table 1: Lattice results for $\left[a_\mu^{\rm SIB}\right]_{\rm conn}$ and $\left[a_\mu^{\rm SIB}\right]_{\rm disc}$, in units of 10^{-10}. The * on the disconnected entry from Ref. [46] is a reminder that this result is not a lattice one, but rather an estimate of the $\pi\pi$ contribution to this quantity obtained using NLO PQChPT, to which a 50% uncertainty has been assigned. We remind the reader that, while FV effects are expected to be small for the connected-plus-disconnected sum, this is not true of the individual components, and separate connected and disconnected results should thus not be compared unless obtained from simulations with comparable physical volumes.

$\left[a_\mu^{\rm SIB}\right]_{\rm conn} \times 10^{10}$	$\left[a_\mu^{\rm SIB}\right]_{\rm disc} \times 10^{10}$	Source
9.5(4.5)	—	[47,48]
10.6(8.0)	—	[44]
6.0(2.3)	—	[42]
9.0(1.4)	−6.9(3.5)*	[46]
6.6(0.8)	−4.7(0.9)	[40]

This paper focuses on the strong isospin-breaking (SIB) contribution, $a_\mu^{\rm SIB}$. A number of lattice groups have reported determinations of the connected contribution, $\left[a_\mu^{\rm SIB}\right]_{\rm conn}$ [40,42,44,46,47], but only one, BMW [40], a result for the disconnected contribution, $\left[a_\mu^{\rm SIB}\right]_{\rm disc}$. BMW finds a strong cancellation between $\left[a_\mu^{\rm SIB}\right]_{\rm conn}$ and $\left[a_\mu^{\rm SIB}\right]_{\rm disc}$, a result anticipated in Ref. [46], which studied the $\pi\pi$ contributions to these quantities using partially quenched Chiral Perturbation Theory (PQChPT) and found an exact cancellation of connected and disconnected contributions at next-to-leading (NLO) chiral order. As we will see below, this cancellation is specific to NLO, and does not persist to higher order. Ref. [46] does not provide a lattice determination of $\left[a_\mu^{\rm SIB}\right]_{\rm disc}$, instead using the NLO PQChPT expression for the contribution of the $\pi\pi$ intermediate state as an estimate, assigning to this estimate a 50% uncertainty. Results from the literature for $\left[a_\mu^{\rm SIB}\right]_{\rm conn}$ and $\left[a_\mu^{\rm SIB}\right]_{\rm disc}$ are summarized in Table 1. Note that, while (as will be confirmed below), one expects finite volume (FV) effects to be small in the full connected-plus-disconnected SIB sum, this is not the case for the individual connected and disconnected components, and significant FV effects are, in fact, observed in the results for $\left[a_\mu^{\rm SIB}\right]_{\rm conn}$ reported in Refs. [42,44,46].

In view of the inflation of the relative error in lattice determinations of $a_\mu^{\rm SIB}$ expected from the strong cancellation between connected and disconnected contributions, an independent, continuum estimate of this quantity is of interest. In this paper, we provide such an estimate using $SU(3)$ chiral perturbation theory (ChPT).

The rest of the paper is organized as follows. In Section 2 we set notation, provide the explicit expression for $a_\mu^{\rm SIB}$ as a weighted integral over Euclidean Q^2 of the IB part of the subtracted EM vacuum polarization, $\hat{\Pi}^{\rm SIB}(Q^2)$, and discuss the features of this expression which make a ChPT estimate of $a_\mu^{\rm SIB}$ feasible. In Section 3, we provide the explicit form of the ChPT representation of $\hat{\Pi}^{\rm SIB}(Q^2)$ needed as input to this expression, and outline the flavor-breaking hadronic τ decay sum rule analysis used to determine the input value for a key higher-order low-energy constant (LEC) needed to encode the effect of ρ-ω mixing. This section also contains our numerical results for $a_\mu^{\rm SIB}$. Finally, Section 4 contains a discussion of these results and our conclusions.

2 The Euclidean integral representation of $a_\mu^{\rm SIB}$ and feasibility of a ChPT determination

In what follows, the vector-current two-point functions, $\Pi^{ab}_{\mu\nu}$, and associated scalar vacuum polarizations, Π^{ab}, are defined, as usual, by

$$\Pi^{ab}_{\mu\nu}(q) = (q_\mu q_\nu - q^2 g_{\mu\nu})\Pi^{ab}(Q^2) = i\int d^4x e^{iq\cdot x}\langle 0|T\{V^a_\mu(x)V^b_\nu(0)\}|0\rangle\,, \tag{1}$$

where $Q^2 \equiv -q^2 \equiv -s$, and V^a_μ are the members of the $SU(3)_F$ octet of vector currents,

$$V^a_\mu = \bar{q}\frac{\lambda^a}{2}\gamma_\mu q\,. \tag{2}$$

The sum of the u, d and s contributions to the electromagnetic (EM) current then has the standard decomposition,

$$J^{EM}_\mu = V^3_\mu + \frac{1}{\sqrt{3}}V^8_\mu\,, \tag{3}$$

into $I=1$ ($a=3$) and $I=0$ ($a=8$) contributions, and the vacuum polarization, $\Pi_{EM}(Q^2)$, of the two-point function of this current the decomposition,

$$\Pi_{EM}(Q^2) = \Pi^{33}(Q^2) + \frac{2}{\sqrt{3}}\Pi^{38}(Q^2) + \frac{1}{3}\Pi^{88}(Q^2)\,, \tag{4}$$

into pure isovector ($ab=33$), pure isoscalar ($ab=88$), and mixed isospin ($ab=38$) parts. Since strong isospin-breaking (SIB) is associated with the $I=1$, $O(m_d-m_u)$ component of the $n_f=3$ QCD mass operator, SIB occurs, to leading order in m_d-m_u, only in the 38 part of Π_{EM}.

The resulting leading order, $O(m_d-m_u)$ SIB component of the EM current vacuum polarization is then

$$\Pi^{\rm SIB}(Q^2) = \frac{2}{\sqrt{3}}\Pi^{38}_{\rm QCD}(Q^2)\,, \tag{5}$$

where the QCD subscript on the right-hand side denotes the $O(m_d-m_u)$ QCD contribution and will be dropped in what follows.

2.1 The Euclidean Q^2 integral representation of $a_\mu^{\rm SIB}$

The full LO, HVP contribution, $a_\mu^{\rm LO,HVP}$, is given, in the Euclidean momentum-squared, Q^2, representation of Refs. [37,38], by the weighted integral

$$a_\mu^{\rm LO,HVP} = -4\alpha^2\int_0^\infty dQ^2 f(Q^2)\hat{\Pi}_{EM}(Q^2)\,, \tag{6}$$

with $\hat{\Pi}_{EM}$ the subtracted EM vacuum polarization defined above, α the EM fine structure constant, and $f(Q^2)$ the exactly known kernel

$$f(Q^2) = m_\mu^2 Q^2 Z^3\,\frac{[1-Q^2Z]}{1+m_\mu^2Q^2Z^2}\,, \tag{7}$$

where

$$Z = \frac{\sqrt{Q^4+4m_\mu^2Q^2}-Q^2}{2m_\mu^2Q^2}\,. \tag{8}$$

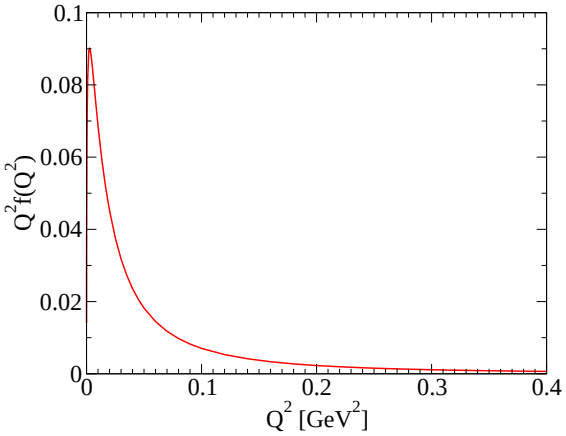

Figure 1: The product $Q^2 f(Q^2)$, with $f(Q^2)$ the weight appearing in the Euclidean integral representation, Eq. (6), of $a_\mu^{\rm LO,HVP}$.

For use in the discussion below, it is convenient to also define the related quantity, $a_\mu^{\rm LO,HVP}(Q^2_{max})$, obtained by replacing the upper limit of the integral in Eq. (6) by Q^2_{max}.

The kernel $f(Q^2)$ diverges as $1/\sqrt{Q^2}$ as $Q^2 \to 0$ and falls rapidly with increasing Q^2, creating a peak in the integrand of Eq. (6) at very low $Q^2 \simeq m_\mu^2/4$. At such low Q^2, $\hat\Pi_{EM}(Q^2)$ should be very close to linear in Q^2, an expectation born out by an evaluation of $\hat\Pi_{EM}(Q^2)$ using $R(s)$ results from Ref. [11] as input to the subtracted dispersive representation

$$\hat\Pi_{EM}(Q^2) = -\frac{Q^2}{12\pi^2}\int_0^\infty ds\,\frac{R(s)}{s(s+Q^2)}\,. \tag{9}$$

The location of the peak of the integrand in Eq. (6) is thus essentially just that of the maximum of the product $Q^2 f(Q^2)$. Figure 1 shows the behavior of this product as a function of Q^2. Note that an analogous figure for $\hat\Pi_{EM}(Q^2) f(Q^2)$, taking into account the deviation from linearity of $\hat\Pi_{EM}(Q^2)$ in the higher-Q^2 region, would show an additional suppression, increasing with Q^2, of contributions at higher Q^2 relative to those from the region of the peak.

The SIB contribution, $a_\mu^{\rm SIB}$ is, similarly, given, in the Euclidean-Q^2 integral representation, by

$$a_\mu^{\rm SIB} = -4\alpha^2\int_0^\infty dQ^2 f(Q^2)\hat\Pi^{\rm SIB}(Q^2)\,. \tag{10}$$

As for $\hat\Pi_{EM}(Q^2)$, $\hat\Pi^{\rm SIB}(Q^2)$ will be very close to linear in Q^2 in the low-Q^2 region, and the maximum of the integrand in Eq. (10) will thus also occur at $Q^2 \simeq m_\mu^2/4$.

2.2 The feasibility of a ChPT determination

The fact that the contributions to the integral representation in Eq. (10) are concentrated at low Q^2 raises the possibility that a reliable estimate of $a_\mu^{\rm SIB}$ might be obtained using the ChPT representation of $\hat\Pi^{\rm SIB}(Q^2)$. An estimate of how reliable such a determination might be can be obtained by studying the related $\hat\Pi^{33}(Q^2)$ case.

The utility of this estimate is based on the following similarities between the spectral functions, $\rho^{38}(s)$ and $\rho^{33}(s)$, of $\Pi^{38}(Q^2)$ and $\Pi^{33}(Q^2)$. First, $\rho^{38}(s)$ and $\rho^{33}(s)$ share a common threshold, $s = 4m_\pi^2$, as well as a common saturation of the low-s region by contributions from $\pi\pi$ intermediate states. Second, while $\rho^{33}(s)$ is necessarily ≥ 0 for all s, while $\rho^{38}(s)$ is not,

the chiral representation of $\rho^{38}(s)$ shows $\rho^{38}(s)$ to be, like $\rho^{33}(s)$, positive in the low-s $\pi\pi$ region. Third, both $\rho^{33}(s)$ and $\rho^{38}(s)$ show sizeable resonance enhancements in the ρ-ω region, as evidenced by the large ρ peak in the $e^+e^- \to \pi^+\pi^-$ cross sections and the obvious IB interference shoulder, centered at $s = m_\omega^2$, on the upper side of that peak. The ρ contribution to $\rho^{33}(s)$ is, of course, positive, while the ρ-ω interference contribution to $\rho^{38}(s)$ has a dispersive shape, with an important contribution which changes sign between $s < m_\omega^2$ and $s > m_\omega^2$.[2] Fits in the interference region using various phenomenological models allow one to obtain model-dependent separations of the isospin-conserving (IC) 33 and IB 38 parts of the $\pi\pi$ cross sections. These can be converted to the corresponding IC and IB contributions to $R(s)$ and the resulting IB contributions integrated with the $a_\mu^{\rm LO,HVP}$ dispersive weight to obtain model-dependent estimates of the IB ρ-ω interference region contribution to $a_\mu^{\rm LO,HVP}$. Such estimates were obtained for a range of models in Refs. [52–56]. Strong cancellations produced by the change of sign noted above and the narrowness of the interference region enhance the model dependence of the associated interference region contribution to $a_\mu^{\rm SIB}$ [52–54]. The sign of the integrated result is, however, positive, and hence the same as that of the IC ρ contribution to $a_\mu^{\rm LO,HVP}$. Integrating, instead, with the weight appearing in the subtracted dispersive representation, Eq. (9), one finds, similarly, a common sign for the IC ρ contribution to $\hat\Pi_{EM}(Q^2)$ and the IB ρ-ω interference region contribution to $\hat\Pi^{\rm SIB}(Q^2)$. From the point of view of $\hat\Pi^{\rm SIB}(Q^2)$ in the spacelike, $Q^2 > 0$ region, the narrow ρ-ω interference contribution to $\rho^{38}(s)$ is essentially indistinguishable from that of a narrow, averaged positive contribution located at $s = m_\omega^2$. As far as the subtracted polarizations are concerned, the spectral functions $\rho^{33}(s)$ and $\rho^{38}(s)$ are thus close analogues of one another all the way from threshold through the first resonance region, and a study of the features of the IC 33 contribution to the representation Eq. (6) can be used to obtain plausible expectations for the behavior of the corresponding representation, Eq. (10), of $a_\mu^{\rm SIB}$.

This observation is of practical use because, in the isospin limit, $\hat\Pi^{33}(Q^2) = \frac{1}{2}\hat\Pi_{ud;V}(Q^2)$, where $\hat\Pi_{ud;V}(Q^2)$ is the subtracted polarization of the flavor ud, $I = 1$, vector current, whose spectral function, $\rho_{ud;V}(s)$, has been extracted from measured differential non-strange hadronic τ decay distributions by ALEPH [57, 59, 60] and OPAL [58]. A version of $\hat\Pi_{ud;V}(Q^2)$ based on the OPAL results for $\rho_{ud;V}(s)$ and the subtracted dispersive representation, was constructed in Ref. [61] and used to study (i) the convergence of $a_\mu^{\rm LO,HVP}(Q^2_{max})$ to the full IC $I = 1$ result, $a_\mu^{\rm LO,HVP}$, as Q^2_{max} was increased from zero to infinity, and (ii) the utility of various representations (including the ChPT representation) of $\hat\Pi_{ud;V}(Q^2)$ in the low-Q^2 region [61, 62]. It was found that $\sim 82\%$ of the $a_\mu^{\rm LO,HVP}$ arises from $Q^2 < 0.10\ GeV^2$, $\sim 92\%$ from $Q^2 < 0.2\ GeV^2$, and $\sim 94\%$ from $Q^2 < 0.25\ GeV^2 \simeq m_K^2$.[3] With the region between $Q^2 = 0$ and m_K^2 plausibly in the range of validity of $SU(3)_F$ ChPT, we thus expect that a determination of $a_\mu^{\rm SIB}$ obtained using ChPT for $\hat\Pi^{\rm SIB}(Q^2)$ and truncating the integral in Eq. (10) at $Q^2_{max} = 0.25\ GeV^2 \simeq m_K^2$ will miss only $\sim 6\%$ of the total contribution to $a_\mu^{\rm SIB}$, provided the ChPT representation used is accurate over this integration region.

The OPAL-based version of $\hat\Pi^{33}(Q^2)$ constructed in Ref. [61] can also be used to explore the accuracy of results obtained using the ChPT representations of subtracted vector current polarizations in the region up to $Q^2 \simeq m_K^2$. To make a sensible estimate of the $I = 1$ (33) contribution to $a_\mu^{\rm LO,HVP}$, the chiral order at which the representation of $\hat\Pi^{33}(Q^2)$ is truncated must be high enough to ensure the effect of the large ρ peak in $\rho^{33}(s)$ is incorporated. This contribution first appears in the chiral expansion through the next-to-next-to-leading-order (NNLO)

[2] See, e.g., Eq. (19), of Ref. [53].

[3] See Figures 1 and 2 of Ref. [62] for plots showing the behavior of $f(Q^2)\hat\Pi_{ud;V}(Q^2)$ as a function of Q^2 and $a_\mu^{\rm LO,HVP;33}(Q^2_{max}) \equiv a_\mu^{33}(Q^2_{max})$ as a function of Q^2_{max}. Note that the quantity denoted $\hat\Pi_{ud;V}(Q^2)$ in Ref. [62] is $\Pi_{ud;V}(0) - \Pi_{ud;V}(Q^2)$, and hence differs by an overall sign from that used in the current paper.

LEC, C_{93}, necessitating the use of the two-loop (NNLO) expression for $\hat{\Pi}^{33}(Q^2)$. Using this representation, with the value of the renormalized LEC $C^r_{93}(0.77\ GeV)$ from Ref. [63] as input, one finds an NNLO ChPT estimate for $a_\mu^{33}(0.25\ GeV^2)$ which overshoots that produced by the OPAL-based version of $\hat{\Pi}^{33}(Q^2)$ by $\sim 4.8\%$. This slight over-shooting is a consequence of the fact that the NNLO representation of $\hat{\Pi}^{33}(Q^2)$ misses small, yet-higher-order contributions of the ρ peak to the curvature of $\hat{\Pi}^{33}(Q^2)$ in the low-Q^2 region. The positivity of the ρ contributions to $\rho^{33}(s)$ ensures that these contributions would, if included, decrease the magnitude of the resulting representation of $\hat{\Pi}^{33}(Q^2)$, producing a result for $a_\mu^{33}(0.25\ GeV^2)$ lower than that given by the NNLO representation. The (overshooting) effect of the truncation at NNLO and the (undershooting) effect of omitting contributions from $Q^2 > 0.25\ GeV^2$ thus work in opposite directions. The NNLO ChPT estimate, $a_\mu^{33}(0.25\ GeV^2)$, is, in fact, only $\sim 1.5\%$ below the full ($Q^2_{max} \to \infty$) $I = 1$ contribution to $a_\mu^{\rm LO,HVP}$ implied by the OPAL-based dispersive version of $\hat{\Pi}^{33}(Q^2)$.

As we will see below, the ChPT result for $a_\mu^{\rm SIB}(0.25\ GeV^2)$ is also dominated by the contribution of a higher-order LEC encoding resonance-region (in this case ρ-ω) effects. Since, as noted above, the contribution of the ρ-ω interference region to the dispersive representation of $\hat{\Pi}^{\rm SIB}(Q^2)$ is equivalent to that of a narrow, net positive contribution to $\rho^{38}(s)$ located at $s = m_\omega^2$, the effect of similarly missing resonance-region-induced, higher-order contributions to the low-Q^2 curvature of $\hat{\Pi}^{\rm SIB}(Q^2)$ will be such that our ChPT estimate for $a_\mu^{\rm SIB}(0.25\ GeV^2)$ will also slightly overshoot the true value of this quantity. There will thus, as in the case of the NNLO result for $a_\mu^{33}(0.25\ GeV^2)$, be a cancellation between the overshooting produced by the use of the truncated ChPT representation and the undershooting caused by the truncation of the integral representation at $Q^2_{max} = 0.25\ GeV^2$. In the analogous a_μ^{33} case, these effects are $O(+5\%)$ and $O(-6\%)$, respectively. Based on these observations, we expect the combination of the truncation in chiral order and truncation of the integral representation at $Q^2 = 0.25\ GeV^2$ to produce an uncertainty of a few to several % in the truncated-in-chiral-order, $a_\mu^{\rm SIB}(0.25\ GeV^2)$ estimate for $a_\mu^{\rm SIB}$ obtained below. To be conservative, since this estimate for the uncertainty relies on results for the analogous, but not identical, a_μ^{33} case, we assign a significantly expanded 10% estimate for the contribution of these effects to the uncertainty on the ChPT-based $a_\mu^{\rm SIB}(0.25\ GeV^2)$ estimate for $a_\mu^{\rm SIB}$.

3 The ChPT estimate for $\hat{\Pi}^{\rm SIB}(Q^2)$

3.1 $\hat{\Pi}^{\rm SIB}(Q^2)$ to two loops in ChPT

The forms of the effective $SU(3)_F$ chiral Lagrangian to NLO and NNLO were worked out long ago in Refs. [64] and [65, 66]. The two-loop (NNLO) representation for the unsubtracted version of the IB polarization, $\Pi^{38}(Q^2)$, can be found in Ref. [67]. From this expression one finds, recasting the result in terms of the Euclidean variable $Q^2 = -q^2$, the following result for the subtracted version, $\hat{\Pi}^{38}(Q^2)$:

$$\hat{\Pi}^{38}(Q^2) = \frac{\sqrt{3}}{4}(m^2_{K^0} - m^2_{K^+})_{\rm QCD}\left[\frac{2i\bar{B}(\bar{m}_K^2, Q^2)}{Q^2} - \frac{1}{48\pi^2\bar{m}_K^2} + \frac{8i\bar{B}(\bar{m}_K^2, Q^2)}{f_\pi^2}\left(\frac{i}{2}\bar{B}_{21}(m_\pi^2, Q^2) + i\bar{B}_{21}(\bar{m}_K^2, Q^2) + \frac{\log\left(m_\pi^2\bar{m}_K^4/\mu^6\right)}{384\pi^2} - L_9^r(\mu)\right)\right], \quad (11)$$

where $(m^2_{K^0} - m^2_{K^+})_{\rm QCD}$ is the non-EM contribution to the kaon mass-squared splitting, $\bar{m}_K^2$ is the non-EM part of the average physical kaon squared mass, $(m^2_{K^0} + m^2_{K^+})/2$, L_9^r is the usual renormalized NLO LEC of Gasser and Leutwyler [64], μ is the chiral renormalization scale,

$\bar{B}(m^2,Q^2)$ is the standard subtracted, equal-mass, two-propagator loop function, given, for $Q^2>0$, by

$$\bar{B}(m^2,Q^2)=\frac{i}{8\pi^2}\left[1-\sqrt{1+4m^2/Q^2}\tanh^{-1}\left(\frac{1}{\sqrt{1+4m^2/Q^2}}\right)\right], \tag{12}$$

and $\bar{B}_{21}$ is the auxillary loop function

$$\bar{B}_{21}(m^2,Q^2)=\frac{1}{12}\left(1+\frac{4m^2}{Q^2}\right)\bar{B}(m^2,Q^2)-\frac{i}{576\pi^2}\,. \tag{13}$$

Our convention for the pion decay constant is that used in Ref. [64], $f_\pi\simeq 92\ MeV$. The first line of Eq. (11) contains the NLO contributions, the second line the NNLO contributions. The low-Q^2 expansion,

$$\frac{2i\bar{B}(m^2,Q^2)}{Q^2}=\frac{1}{48\pi^2m^2}+O(Q^2), \tag{14}$$

has been used in obtaining the subtracted form, Eq. (11), from the unsubtracted form given in Ref. [67]. The absence of an NLO pion loop contribution in Eq. (11) reflects the cancellation noted in Ref. [46] between NLO $\pi\pi$ intermediate state contributions to the connected and disconnected parts of $\hat{\Pi}^{38}$. The presence of the pion loop function factor, $\bar{B}_{21}(m_\pi^2,Q^2)$, in the NNLO expression shows this cancellation does not persist beyond NLO. The result $L_9^r(\mu=0.77\ GeV)=0.00593(43)$ from Ref. [68] is used in obtaining numerical results below.

As is well known, the separation of IB effects into strong and EM contributions is ambiguous at $O(\alpha(m_d+m_u))$.[4] Since m_d-m_u and m_d+m_u differ by only a factor of ~ 3 for physical m_u and m_d, this ambiguity is, in fact, at the level of effects second order in IB, which we are neglecting. The impact of this ambiguity, in any case, lies essentially entirely in the factor $(m_{K^0}^2-m_{K^+}^2)_{\rm QCD}$ in Eq. (11). At leading order in IB, this factor can be determined by subtracting the EM contribution to the K mass-squared splitting. This is related to the EM contribution to the pion mass-squared splitting by

$$(m_{K^+}^2-m_{K^0}^2)_{\rm EM}=(m_{\pi^+}^2-m_{\pi^0}^2)_{EM}\,(1+\epsilon_D)\,, \tag{15}$$

where ϵ_D (which depends on the light quark masses and the strong-EM separation scheme choice) parametrizes the breaking of Dashen's Theorem [70], and is equal to zero in the $SU(3)$ chiral limit. Since the experimental pion mass-squared splitting receives no SIB contribution at $O(m_d-m_u)$, $(m_{\pi^+}^2-m_{\pi^0}^2)_{EM}$ can, up to corrections second order in IB, be replaced by the corresponding experimental value. Using the FLAG 2019 [69] $n_f=2+1+1$ result, $\epsilon_D=0.79(7)$, as input, we find

$$(m_{K^0}^2-m_{K^+}^2)_{\rm QCD}=0.00616(9)\ GeV^2\,, \tag{16}$$

a result valid to first order in IB.

Inputting the NNLO representation of $\hat{\Pi}^{38}(Q^2)$ given by Eq. (11) into Eq. (10), and using the numerical input specified above, one finds the following results for the NLO and NNLO contributions to $a_\mu^{\rm SIB}(0.25\ GeV^2)$:

$$\left[a_\mu^{\rm SIB}(0.25\ GeV^2)\right]_{\rm NLO}=0.073\times10^{-10}\,, \tag{17}$$

$$\left[a_\mu^{\rm SIB}(0.25\ GeV^2)\right]_{\rm NNLO}=0.552(37)\times10^{-10}\,, \tag{18}$$

where the error on the NNLO contribution is that induced by the uncertainty on the input for $L_9^r(0.77\ GeV)$. The smallness of the NLO contribution in Eq. (17) is a reflection of the exact

[4] A particularly clear discussion of this point is given in Sections 3.1.1 and 3.1.2 of the 2019 FLAG report [69].

cancellation at NLO between connected and disconnected contributions from $\pi\pi$ intermediate states. The total to NNLO,

$$\left[a_\mu^{\rm SIB}(0.25\ GeV^2)\right]_{\rm NLO+NNLO} = 0.625(37)\times 10^{-10}\,, \tag{19}$$

is also small, and dominated by the unsuppressed NNLO contribution. The smallness of the NLO+NNLO total should come as no surprise since no LEC encoding resonance-region ρ-ω interference contributions to $\hat{\Pi}^{38}(Q^2)$ appears in the NNLO representation Eq. (11). The situation is analogous to that of the ChPT representation of $\hat{\Pi}^{33}(Q^2)$, where the LEC, C_{93}, which encodes the dominant ρ contribution, does not appear in the NLO representation. The next subsection addresses this shortcoming of the NNLO representation of $\hat{\Pi}^{38}(Q^2)$ and shows how results from flavor-breaking hadronic τ decay sum rules can be used to quantify the dominant contribution to $a_\mu^{\rm SIB}$ from terms beyond NNLO in the chiral expansion.

3.2 Contributions to $\hat{\Pi}^{\rm SIB}(Q^2)$ beyond two loops

The mesonic low-energy effective Lagrangian of ChPT has as explicit degrees of freedom only the low-lying, pseudoscalar mesons. The effects of resonance degrees of freedom, which have been integrated out, are encoded in the LECs of the effective theory. As is well known, contributions from the lowest-lying resonances provide estimates for these LECs which typically agree well with phenomenological determinations [71].

At low Q^2, the ρ-ω mixing contribution to ρ^{38} produces a leading low-Q^2 contribution to $\hat{\Pi}^{38}(Q^2)$ of the form $C_{\rho\omega}Q^2$ where $C_{\rho\omega}$ is a constant proportional to the product $f_\rho f_\omega \theta_{\rho\omega}$, with f_ρ the ρ decay constant (which parametrizes the ρ coupling to J_μ^3), f_ω the ω decay constant (which parametrizes the ω coupling to J_μ^8) and $\theta_{\rho\omega}$ the IB parameter characterizing the strength of ρ-ω mixing. No tree-level contribution of the form CQ^2 appears in the NNLO expression Eq. (11), establishing that ρ-ω mixing effects are not yet encoded in the NNLO form. The reason for this absence is obvious. An operator in the effective Lagrangian producing an SIB, tree-level CQ^2 contribution to $\hat{\Pi}^{38}(Q^2)$ would have to include one factor of the quark mass matrix and four derivatives (two to produce the factor $(q_\mu q_\nu - g_{\mu\nu}q^2)$ in $\Pi_{\mu\nu}^{38}$ and two to produce the Q^2 in the CQ^2 contribution to $\hat{\Pi}^{38}(Q^2)$). Such an operator is next-to-next-to-next-to-leading-order (NNNLO) in the chiral counting. The LECs encoding the effects of ρ-ω mixing (as well as of all other higher-energy degrees of freedom integrated out in forming the effective Lagrangian) thus do not appear in the chiral expansion of $\hat{\Pi}^{38}(Q^2)$ until NNNLO.

Model-dependent results for the contribution to $a_\mu^{\rm SIB}$ from the ρ-ω interference region can, of course, be obtained using experimental results for the $\pi\pi$ cross-sections in the interference region and separations of the IC and IB contributions to these cross sections produced by fits based on phenomenological models of the pion form factor $F_\pi(s)$. Such results, of course, provide no information about NNNLO (and higher) contributions to $a_\mu^{\rm SIB}$ from other high-energy degrees of freedom also integrated out in forming the effective Lagrangian, though they do serve to provide an estimate of the expected scale of NNNLO and higher order contributions. The resulting ρ-ω interference region contributions are a factor ~ 4 or more times larger than the NLO+NNLO result (19), confirming the numerical importance of beyond-NNLO contributions. Contributions other than that induced by ρ-ω mixing, for example due to ρ'-ω' mixing, are, of course, also expected at some level. With the ρ' and ω' having comparable widths, and no analogue of the ρ-ω interference shoulder evident in the $\pi\pi$ cross-sections in the ρ'-ω' region, no similar phenomenological estimate is possible for such higher resonance contributions.

An advantage of the chiral representation of the low-Q^2 contributions to $a_\mu^{\rm SIB}$ is that contributions from all degrees of freedom integrated out in forming the effective Lagrangian, not just

those from the ρ-ω interference region, will be encoded in the relevant NNNLO (and higher) LECs. It turns out that, at NNNLO, there is only one such LEC, denoted $\delta C_{93}^{(1)}$ in Ref. [63]. The normalization is such that, retaining only vector external sources, $v_\mu = v_\mu^a \lambda^a/2$, quark-mass-dependent tree-level NNNLO contributions to all octet vector-current two-point functions are generated by the effective NNNLO operator

$$8B_0 Q^2 \delta C_{93}^{(1)} \mathrm{Tr}[M v^\mu v^\nu] \left(q_\mu q_\nu - g_{\mu\nu} q^2\right), \tag{20}$$

where M is the quark mass matrix and B_0 the standard leading-order (LO) LEC, related to the chiral limit value of the quark condensate.[5] The tree-level contribution to $\Pi_{\mu\nu}^{38}$ and thence to $\hat{\Pi}^{38}$ is obtained by taking the second derivative of this expression with respect to v_μ^3 and v_ν^8. An estimate of beyond-NNLO contributions to $a_\mu^{\rm SIB}$ thus requires only a determination of the LEC $\delta C_{93}^{(1)}$.

The situation for the chiral representation of $a_\mu^{\rm SIB}$ is similar to that of the chiral representation of the $I = 1$ ($ab = 33$) contribution to $a_\mu^{\rm LO,HVP}$, where the leading (tree-level LEC) contribution from the ρ resonance enters beginning only at NNLO. The NLO representation thus produces a dramatic underestimate of $a_\mu^{\rm LO,HVP;33}$. As noted above, this underestimate is almost completely cured once NNLO contributions, including, in particular, the ρ-dominated contribution proportional to C_{93}, are included.

It turns out that the NNNLO LEC, $\delta C_{93}^{(1)}$, which encodes the contributions to $a_\mu^{\rm SIB}$, at NNNLO, from all degrees of freedom integrated out in forming the effective Lagrangian (including those from the ρ-ω interference region) has already been determined in a flavor-breaking (FB), inverse-moment finite-energy sum rule (IMFESR) analysis of non-strange and strange hadronic τ decay distribution data [63]. We outline this determination below, and provide a numerical update of its results for $\delta C_{93}^{(1)}$.

FB hadronic τ data can be used to determine $\delta C_{93}^{(1)}$ because of the close relation between $\hat{\Pi}^{38}(Q^2)$ and the FB vector current combination $\hat{\Pi}_{ud-us;V}(Q^2) \equiv \hat{\Pi}_{ud;V}(Q^2) - \hat{\Pi}_{us;V}(Q^2)$.[6] $\hat{\Pi}_{ud-us;V} = \hat{\Pi}^{11} + \hat{\Pi}^{22} - \hat{\Pi}^{44} - \hat{\Pi}^{55}$, and hence involves symmetric products of flavor-octet vector currents. The FB component of the QCD quark mass operator,

$$\frac{-2}{\sqrt{3}}(m_s - m_u - m_d)\bar{q}\frac{\lambda^8}{2}q, \tag{21}$$

is proportional to the $a = 8$ member of the flavor octet, $S^a = \bar{q}\frac{\lambda^2}{2}q$, of light-quark scalar densities. The FB combination $\hat{\Pi}_{ud-us;V}$ thus, to first order in FB, is determined by the $a = 8$ member of the symmetric 8_F multiplet of the products of octet vector currents. Since the SIB component of the QCD quark mass operator,

$$-(m_d - m_u)\bar{q}\frac{\lambda^3}{2}q, \tag{22}$$

is proportional to the $a = 3$ member of the same octet of scalar densities, and $\Pi_{\mu\nu}^{38}$ involves the symmetric product, $J_\mu^3 J_\nu^8 + J_\mu^8 J_\nu^3$, of two members of the same octet of vector currents,

[5] In terms of the $N_f = 3$ labelling of the basis of operators for the general NNNLO effective Lagrangian constructed in Ref. [72], the operators generating the term (20) are numbers 944 and 945, both of which reduce to the form entering (20) when only external vector sources are present and only tree-level, vector-current two-point function contributions are considered.

[6] Since $m_s \neq m_u$, the flavor us vector current is not conserved. The associated two-point function thus has non-zero spin $J = 1$ and 0 vaccum polarizations, each of which has a kinematic singularity at $Q^2 = 0$. As usual, these singularities cancel in the $J = 0 + 1$ sum, and by $\hat{\Pi}_{us;V}(Q^2)$ we mean the subtracted version of the kinematic-singularity-free sum of the $J = 0$ and 1 polarizations.

$\hat{\Pi}^{38}$, is determined, to first order in SIB, by the $a = 3$ member of the same symmetric 8_F multiplet of products of the octet vector currents. A determination of the contributions beyond NNLO to $\hat{\Pi}_{ud-us;V}$ will thus, up to corrections higher order in $SU(3)_F$ breaking, also provide a determination of the contributions beyond NNLO to $\hat{\Pi}^{38}$.

The NNNLO version of the relation between these two quantities follows immediately from the structure of the NNNLO operator in (20). The FB NNNLO contribution to $\hat{\Pi}_{ud-us;V}(Q^2)$ and SIB NNNLO contribution to $\hat{\Pi}^{\rm SIB}(Q^2)$ produced by this operator are

$$\left[\hat{\Pi}_{ud-us;V}(Q^2)\right]_{\rm NNNLO,LEC} = -8Q^2(m_K^2 - m_\pi^2)\,\delta C_{93}^{(1)}\,, \tag{23}$$

and

$$\left[\hat{\Pi}^{\rm SIB}(Q^2)\right]_{\rm NNNLO,LEC} = -\frac{8}{3}Q^2\left(m_{K^0}^2 - m_{K^+}^2\right)_{\rm QCD}\,\delta C_{93}^{(1)}\,, \tag{24}$$

where the LO relations $B_0(m_s - m_u) = m_K^2 - m_\pi^2$ and $B_0(m_d - m_u) = \left(m_{K^0}^2 - m_{K^+}^2\right)_{\rm QCD}$ have been used to recast the results in terms of pseudoscalar meson masses. While (since they encode resonance-region contributions missing at NNLO) we expect these terms to dominate the contributions beyond NNLO, the argument above shows that the relation between NNNLO and higher FB contributions to $\hat{\Pi}_{ud-us;V}(Q^2)$ and NNNLO and higher SIB contributions to $\hat{\Pi}^{\rm SIB}(Q^2)$ is more general, and extends beyond the relation between the tree-level NNNLO contributions.[7]

We now outline the determination of $\delta C_{93}^{(1)}$ from the FB IMFESR analysis of hadronic τ decay data. This analysis is favored as a means of determining $\delta C_{93}^{(1)}$ because the spectral functions, $\rho_{ud;V}(s)$ and $\rho_{us;V}(s)$, of $\hat{\Pi}_{ud;V}$ and $\hat{\Pi}_{us;V}$ can be determined experimentally, up to $s = m_\tau^2$, from the measured differential non-strange and strange hadronic τ decay distributions [73]. Experimental data can thus be used to evaluate the first term on the right-hand side of the FB IMFESR

$$\left.\frac{d\hat{\Pi}_{ud-us;V}(Q^2)}{dQ^2}\right|_{Q^2=0} = = -\int_{4m_\pi^2}^{s_0} ds\, w_\tau(s/s_0)\,\frac{\rho_{ud;V}(s) - \rho_{us;V}(s)}{s^2} \tag{25}$$

$$-\frac{1}{2\pi i}\oint_{|s|=s_0} ds\, w_\tau(s/s_0)\,\frac{\hat{\Pi}_{ud-us;V}(Q^2=-s)}{s^2}\,, \tag{26}$$

provided $s_0 \leq m_\tau^2$. The operator product expansion (OPE) is used to evaluate the (numerically very small) second term on the right-hand side. The τ kinematic weight factor, $w_\tau(x) = 1 - 3x^2 + 2x^3$, with $x = s/s_0$, has been included (i) because of its double zero at $s = s_0$, which serves to suppress duality violating contributions and improve the accuracy of the OPE approximation [74, 75], and (ii) because its derivative with respect to s at $s = 0$ is 0, which ensures only the derivative of the polarization with respect to Q^2 appears on the left-hand side. Analogous IMFESRs provide the slopes with respect to Q^2, at $Q^2 = 0$, of the separate non-strange and strange polarizations $\hat{\Pi}_{ud;V}$ and $\hat{\Pi}_{us;V}$. The chiral representations of $\hat{\Pi}_{ud;V}(Q^2)$ and $\hat{\Pi}_{us;V}(Q^2)$ are known to NNLO and given in Ref. [76]. Both contain numerically small NLO and NNLO loop contributions and a common, numerically dominant tree-level NNLO LEC contribution $8Q^2C_{93}^r$ encoding the leading ρ contribution to $\hat{\Pi}_{ud;V}(Q^2)$ and K^* contribution to $\hat{\Pi}_{us;V}(Q^2)$. These leading representations of resonance-region effects cancel in the NNLO representation of the FB difference $\hat{\Pi}_{ud-us;V}(Q^2)$. Resonance-region contributions to

[7] This is, for example, true of leading contributions to the curvatures with respect to Q^2 at $Q^2 = 0$, which are generated by terms also involving only a single insertion of the quark mass matrix. The argument, however, does not hold for higher-order contributions generated by terms involving two insertions of the quark mass matrix, which is why the NNNLO relation between the slopes is subject to potential $SU(3)_F$-breaking corrections beyond NNNLO.

$\hat{\Pi}_{ud-us;V}(Q^2)$ thus, as for $\hat{\Pi}^{38}(Q^2)$ (and for the same reason as in the $\hat{\Pi}^{38}(Q^2)$ case) first enter at NNNLO in the chiral expansion. Contributions to the slopes with respect to Q^2 of $\hat{\Pi}_{ud;V}(Q^2)$ and $\hat{\Pi}_{us;V}(Q^2)$ in the low-Q^2 region are expected to be dominated by the effects of the ρ and K^* resonances. Since these contributions produce slopes at $Q^2 = 0$ which, in the narrow width approximation, are proportional to f_ρ^2/m_ρ^4 and $f_{K^*}^2/m_{K^*}^4$, a FB difference of order $\sim 40\%$ between the $\hat{\Pi}_{ud;V}(Q^2)$ and $\hat{\Pi}_{us;V}(Q^2)$ slopes would not be unexpected. A difference of this magnitude is easily determinable from the FB IMFESR, Eq.(26), given the accuracy of current experimental hadronic τ decay distributions.

The slope $\left[d\hat{\Pi}_{ud-us;V}(Q^2)/dQ^2\right]_{Q^2=0}$ was determined in Ref. [63] using then-current OPE input and $\rho_{ud;V}(s)$ and $\rho_{us;V}(s)$ obtained from then-current versions of the non-strange and strange experimental τ decay distributions. Important inputs to this analysis are the exclusive-mode strange τ branching fractions (BFs), which set the overall scales of the corresponding exclusive-mode contributions to $\rho_{us;V}(s)$. At the time of the analysis of Ref. [63], there was a disagreement between the HFAG assessments of the two $\tau \to K\pi\nu_\tau$ BFs and the expectations for these BFs from the dispersive analysis of Ref. [77] (ACLP). Since the sum of these BFs sets the normalization for the dominant $K\pi$ contribution to $\rho_{us;V}(s)$, this disagreement produced a disagreement between results for the FB slope at $Q^2 = 0$ obtained using the HFAG and ACLP $K\pi$ normalizations. Ref. [63] thus quoted two different determinations of the FB slope difference, and hence two different results for $\delta C_{93}^{(1)}$, the latter obtained assuming the slope difference is dominated by the NNNLO contribution.

New experimental information has since resolved the $K\pi$ BF discrepancy in favor of the dispersive ACLP expectation: the sum of the $\tau \to K\pi\nu_\tau$ BFs reported in the 2019 HFLAV compilation [78] agrees well with the ACLP expectation and, in addition, has a significantly smaller uncertainty. We have thus updated the determination of $\delta C_{93}^{(1)}$ in Ref. [63] using (i) current 2019 HFLAV results for all τ BFs and correlations, (ii) the updated determination of $\rho_{ud;V}(s)$ reported in Ref. [79], (iii) updated PDG [80] input for α_s, V_{ud} and V_{us}, (iv) updated 2019 FLAG [69] input for the light-quark masses, and (v) the most recent HPQCD result [81] for the strange-to-light-quark condensate ratio. While included for completeness, updates other than those to the $\tau \to K\pi\nu_\tau$ BFs have negligible impact on the results for the FB slope difference. The updated result,

$$\left.\frac{d\hat{\Pi}_{ud-us;V}(Q^2)}{dQ^2}\right|_{Q^2=0} = -0.0862(24)\ GeV^{-2}, \tag{27}$$

has an improved error and central value very close to the ACLP-based result, $-0.0868(40)\ GeV^{-2}$, of Ref. [63]. The updated slope produces an updated estimate,

$$\delta C_{93}^{(1)}\left(m_K^2 - m_\pi^2\right) = 0.00534(37)\ GeV^{-2}, \tag{28}$$

for the NNNLO LEC $\delta C_{93}^{(1)}$.

Our assessment of the NNNLO contribution to $\hat{\Pi}^{\rm SIB}(Q^2)$ is obtained by substituting Eq. (28) into (24). Weighting this expression with the factor $-4\alpha^2 f(Q^2)$ appearing in Eq. (10) and integrating between $Q^2 = 0$ to $0.25\ GeV^2$ produces our estimate,

$$\left[a_\mu^{\rm SIB}(0.25\ GeV^2)\right]_{\rm NNNLO} = 2.69(19)\times 10^{-10}, \tag{29}$$

for the NNNLO contribution to $a_\mu^{\rm SIB}(0.25\ GeV^2)$, and hence for the NNNLO contribution to $a_\mu^{\rm SIB}$. The error in Eq. (29) reflects only the uncertainty on the input for $\delta C_{93}^{(1)}$ from Eq. (28). We assign an additional $\sim 30\%$ uncertainty to the NNNLO result to account for the absence of small non-resonance-induced NNNLO loop contributions and the impact of possible contributions

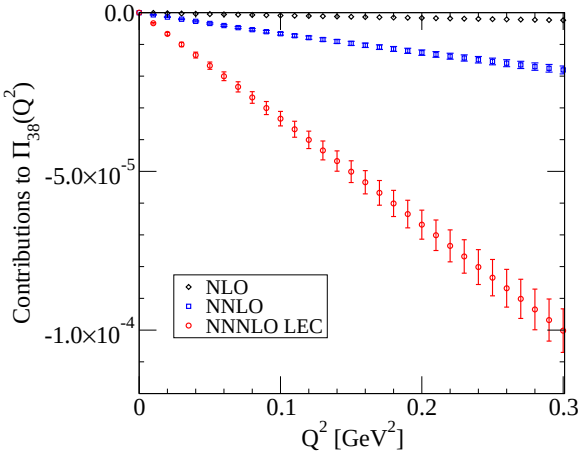

Figure 2: The NLO, NNLO and NNNLO LEC contributions to $\hat{\Pi}^{38}(Q^2)$. The errors on the NNLO and NNNLO LEC points are those induced by the uncertainties on the input value for L_9^r and the contribution to the error on $\delta C_{93}^{(1)}$ quoted in Eq. (28), respectively.

higher order in FB to the slope at $Q^2 = 0$ of $\hat{\Pi}_{ud-us;V}(Q^2)$.[8]

Figure 2 shows the Q^2 dependence of the NLO, NNLO and "NNNLO LEC" contributions to $\hat{\Pi}^{38}(Q^2)$, where "NNNLO LEC" denotes the tree-level contribution proportional to $\delta C_{93}^{(1)}$. It is clear that the NNNLO LEC contribution is numerically dominant, and that, although the loop functions which determine the NLO and NNLO contributions are not strictly linear in Q^2, they are, numerically, very close to being so, in the region of interest to us. The errors on the NNLO and NNNLO LEC contributions are those associated with the uncertainty on the input for L_9^r, and that on the leading-order-in-FB result, Eq. (28), for $\delta C_{93}^{(1)}$.

Adding to the NNNLO LEC result, (29), the NLO and NNLO contributions (17) and (18), we obtain our final estimate for $a_\mu^{\rm SIB}$,

$$a_\mu^{\rm SIB} = 3.32(4)(19)(33)(81) \times 10^{-10}\,, \tag{30}$$

where the first error is that induced on the NNLO contribution by the uncertainty on the input for L_9^r, the second is that associated with the error on the FB IMFESR estimate, Eq. (28), for $\delta C_{93}^{(1)}$, the third is our 10% estimate for the uncertainty produced by the combination of truncating the integral for $a_\mu^{\rm SIB}$ at $Q^2_{max} = 0.25\ GeV^2$ and neglecting contributions beyond NNLO to the curvature of $\hat{\Pi}^{\rm SIB}(Q^2)$, and the fourth is that induced by our $\sim 30\%$ estimate for the uncertainty in $\delta C_{93}^{(1)}$ induced by possible higher-order FB contributions to the slope of $\hat{\Pi}_{ud-us;V}(Q^2)$ at $Q^2 = 0$ obtained from the updated version of the FB IMFESR analysis of Ref. [63].

The NLO, NNLO and NNNLO LEC contributions to $a_\mu^{\rm SIB}[Q^2_{max}]$, together with the NLO+NNLO+NNNLO LEC total, are shown as a function of Q^2_{max} in Figure 3. The shaded band on the total shows the quadrature sum of the LEC-uncertainty-induced NNLO and NNNLO LEC errors plotted in Fig. 2. The dashed and solid horizontal lines show, respectively, the central value and associated $\pm 0.89 \times 10^{-10}$ combined error range of our final result, Eq. (30), the latter obtained by adding in quadrature the four error components from Eq. (30).

[8] The FB IMFESR provides an essentially purely experimental determination of the FB slope difference. The associated determination of $\delta C_{93}^{(1)}$, however, relies on the assumption that this result is dominated by the leading-order-in-FB contribution associated with the NNNLO operator (20). This assumption might be subject to $O(30\%)$ $SU(3)_F$ corrections.

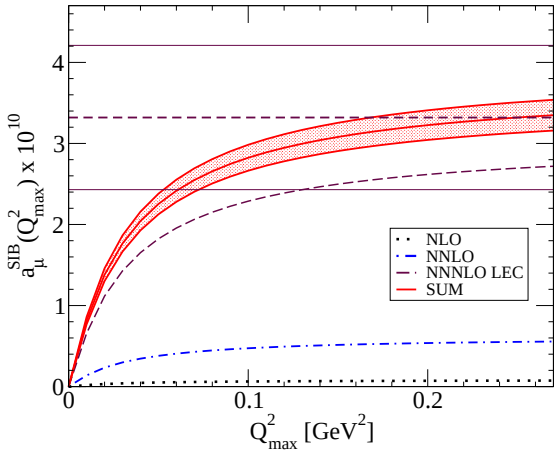

Figure 3: The accumulation of the NLO, NNLO and NNNLO LEC contributions to $a_\mu^{\rm SIB}$ as a function of the upper integration limit, Q^2_{max}. The errors on the NNLO and NNNLO LEC contributions have been suppressed. The shaded band shows the error on the sum of the NLO, NNLO and NNNLO LEC contributions obtained by summing the NNLO and NNNLO LEC errors from Fig. 2 in quadrature. The horizontal dashed line and two solid horizontal lines represent, respectively, the final central value and associated error range specified in Eq. (31).

4 Summary and conclusions

We have obtained a continuum, ChPT-based estimate of the SIB contribution, $a_\mu^{\rm SIB}$, to $a_\mu^{\rm LO,HVP}$, the leading-order, hadronic-vacuum-polarization contribution to the anomalous magnetic moment of the muon. As shown in Figs. 2 and 3, the NLO contribution to this result is very small, presumably as a consequence of the cancellation at this order between disconnected and connected contributions from $\pi\pi$ intermediate states. The NNLO contribution, though significantly larger, is also sub-dominant, a result not unexpected given the absence of terms encoding resonance-region contributions from the NNLO representation. Resonance-region contributions first appear in the chiral expansion of $a_\mu^{\rm SIB}$ at NNNLO, encoded in the NNNLO LEC $\delta C_{93}^{(1)}$. Our full estimate, (30), for $a_\mu^{\rm SIB}$ is thus, as expected, dominated by the NNNLO contribution proportional to $\delta C_{93}^{(1)}$. Fortunately, an estimate for this LEC can be obtained from a FB IMFESR analysis of experimental hadronic τ decay distributions, and we have updated the original version of this analysis, reported in Ref. [63], to take into account subsequent, numerically relevant changes to the normalization of the dominant $K\pi$ contribution to the strange experimental distribution. The resulting NNNLO LEC contribution to $a_\mu^{\rm SIB}$ is similar in size to the results of phenomenological estimates for the contribution from the ρ-ω interference region based on model-dependent fits to experimental interference-region $e^+e^- \to \pi^+\pi^-$ cross sections, confirming the importance of contributions from the ρ-ω region. The ChPT analysis has the advantage, over such phenomenological estimates of the contribution from this one, narrow region only, of including also contributions from the lower-Q^2 region, evaluated in the model-independent chiral framework, as well as those from regions of the spectrum above $s \simeq m_\omega^2$ where the absence of experimentally observable IB interference effects makes analogous phenomenological estimates impossible.

The dominance of the result in Eq. (30) by the NNNLO LEC term in the chiral representation of $\hat{\Pi}^{38}(Q^2)$ and hence by contributions from higher-energy (short-distance) resonance degrees of freedom confirms the expectation that, once connected and disconnected contributions have

been summed, FV effects in lattice determinations of $a_\mu^{\rm SIB}$ will be small, relative to $a_\mu^{\rm SIB}$, and hence can be neglected on the scale of the current precision goal for the determination of $a_\mu^{\rm LO,HVP}$. The situation for the relative size of FV effects should, in fact, be similar to that of the $I = 1$ contribution, a_μ^{33}, where the contribution proportional to the NNLO LEC C_{93} which encodes the higher-energy ρ degree of freedom also dominates the chiral representation. The only difference between the two cases is a practical one: while few-to-several percent FV corrections to the large a_μ^{33} contribution are far from numerically negligible on the scale of the current precision target, analogous few-to-several percent FV corrections to the much (more than two orders of magnitude) smaller SIB contribution are entirely negligible on that same precision target scale.

Our final result, obtained by combining all four errors from Eq. (30) in quadrature, is

$$a_\mu^{\rm SIB} = 3.32(89) \times 10^{-10} \,. \tag{31}$$

The central value is larger than that of the BMW lattice result,

$$\left[a_\mu^{\rm SIB}\right]_{BMW} = 1.93(83)(87) \times 10^{-10} = 1.93(1.20) \times 10^{-10} \,, \tag{32}$$

obtained by summing the connected and disconnected contributions reported in Ref. [40], but compatible with it within errors.[9]

We close by noting that, given the dominance of the result by the contribution proportional to the NNNLO LEC $\delta C_{93}^{(1)}$, and the leading linear-in-Q^2 behavior of this contribution, it would be of interest were future lattice studies to quote results for the slope of $\hat{\Pi}^{\rm SIB}(Q^2)$ with respect to Q^2 at $Q^2 = 0$, a result otainable from the t^4 time moment of the two-point function at zero spatial momentum [82].

Acknowledgments

Funding information The work of C.L.J., R.L. and K.M. is supported by the Natural Sciences and Engineering Research Council of Canada.

References

[1] G. W. Bennett et al., *Measurement of the positive muon anomalous magnetic moment to 0.7 ppm*, Phys. Rev. Lett. **89**, 101804 (2002), doi:10.1103/PhysRevLett.89.101804.

[2] G. W. Bennett et al., *Measurement of the negative muon anomalous magnetic moment to 0.7 ppm*, Phys. Rev. Lett. **92**, 161802 (2004), doi:10.1103/PhysRevLett.92.161802.

[3] G. W. Bennett et al., *Final report of the E821 muon anomalous magnetic moment measurement at BNL*, Phys. Rev. D **73**, 072003 (2006), doi:10.1103/PhysRevD.73.072003.

[4] B. Abi, et al., *Measurement of the positive muon anomalous magnetic moment to 0.46 ppm*, Phys. Rev. Lett. **126**, 141801 (2021), doi:10.1103/PhysRevLett.126.141801.

[5] T. Aoyama et al., *The anomalous magnetic moment of the muon in the Standard Model*, Phys. Rep. **887**, 1 (2020), doi:10.1016/j.physrep.2020.07.006.

[9] The statistical and systematic errors, 0.83×10^{-10} and 0.87×10^{-10}, on the BMW result are the quadrature sums of the corresponding statistical/systematic errors on the connected and disconnected contributions. We thank Laurent Lellouch for clarification on how these errors should be combined.

[6] T. Aoyama, M. Hayakawa, T. Kinoshita and M. Nio, *Complete tenth-order QED contribution to the muon $g-2$*, Phys. Rev. Lett. **109**, 111808 (2012), doi:10.1103/PhysRevLett.109.111808.

[7] T. Aoyama, T. Kinoshita and M. Nio, *Theory of the anomalous magnetic moment of the electron*, Atoms **7**, 28 (2019), doi:10.3390/atoms7010028.

[8] A. Czarnecki, W. J. Marciano and A. Vainshtein, *Refinements in electroweak contributions to the muon anomalous magnetic moment*, Phys. Rev. D **67**, 073006 (2003), doi:10.1103/PhysRevD.67.073006.

[9] C. Gnendiger, D. Stöckinger and H. Stöckinger-Kim, *The electroweak contributions to $(g-2)_\mu$ after the Higgs-boson mass measurement*, Phys. Rev. D **88**, 053005 (2013), doi:10.1103/PhysRevD.88.053005.

[10] M. Davier, A. Hoecker, B. Malaescu and Z. Zhang, *Reevaluation of the hadronic vacuum polarisation contributions to the Standard Model predictions of the muon $g-2$ and $\alpha(m_Z^2)$ using newest hadronic cross-section data*, Eur. Phys. J. C **77**, 827 (2017), doi:10.1140/epjc/s10052-017-5161-6.

[11] A. Keshavarzi, D. Nomura and T. Teubner, *Muon $g-2$ and $\alpha(m_Z^2)$: A new data-based analysis*, Phys. Rev. D **97**, 114025 (2018), doi:10.1103/PhysRevD.97.114025.

[12] M. Davier, A. Hoecker, B. Malaescu and Z. Zhang, *A new evaluation of the hadronic vacuum polarisation contributions to the muon anomalous magnetic moment and to $\alpha(m_Z^2)$*, Eur. Phys. J. C **80**, 241 (2020), doi:10.1140/epjc/s10052-020-7792-2.

[13] A. Keshavarzi, D. Nomura and T. Teubner, *$g-2$ of charged leptons, $\alpha(m_Z^2)$, and the hyperfine splitting of muonium*, Phys. Rev. D **101**, 014029 (2020), doi:10.1103/PhysRevD.101.014029.

[14] G. Colangelo, M. Hoferichter and P. Stoffer, *Two-pion contribution to hadronic vacuum polarization*, J. High Energy Phys. **02**, 006 (2019), doi:10.1007/JHEP02(2019)006.

[15] M. Hoferichter, B.-L. Hoid and B. Kubis, *Three-pion contribution to hadronic vacuum polarization*, J. High Energy Phys. **08**, 137 (2019), doi:10.1007/JHEP08(2019)137.

[16] A. Kurz, T. Liu, P. Marquard and M. Steinhauser, *Hadronic contribution to the muon anomalous magnetic moment to next-to-next-to-leading orde*, Phys. Lett. B **734**, 144 (2014), doi:10.1016/j.physletb.2014.05.043.

[17] K. Melnikov and A. Vainshtein, *Hadronic light-by-light scattering contribution to the muon anomalous magnetic moment reexamined*, Phys. Rev. D **70**, 113006 (2004), doi:10.1103/PhysRevD.70.113006.

[18] P. Masjuan and P. Sanchez-Puertas, *Pseudoscalar-pole contribution to the $(g_\mu-2)$: A rational approach*, Phys. Rev. D **95**, 054026 (2017), doi:10.1103/PhysRevD.95.054026.

[19] G. Colangelo, M. Hoferichter, M. Procura and P. Stoffer, *Dispersion relation for hadronic light-by-light scattering: Two-pion contributions*, J. High Energy Phys. **04**, 161 (2017), doi:10.1007/JHEP04(2017)161.

[20] M. Hoferichter, B.-L. Hoid, B. Kubis, S. Leupold and S. P. Schneider, *Dispersion relation for hadronic light-by-light scattering: Pion pole*, J. High Energy Phys. **10**, 141 (2018), doi:10.1007/JHEP10(2018)141.

[21] A. Gérardin, H. B. Meyer and A. Nyffeler, *Lattice calculation of the pion transition form factor with Wilson quarks*, Phys. Rev. D **100**, 034520 (2019), doi:10.1103/PhysRevD.100.034520.

[22] J. Bijnens, N. Hermansson-Truedsson and A. Rodríguez-Sánchez, *Short-distance constraints for the HLbL contribution to the muon anomalous magnetic moment*, Phys. Lett. B **798**, 134994 (2019), doi:10.1016/j.physletb.2019.134994.

[23] G. Colangelo, F. Hagelstein, M. Hoferichter, L. Laub and P. Stoffer, *Longitudinal short-distance constraints for the hadronic light-by-light contribution to $(g-2)_\mu$ with large-N_c Regge models*, J. High Energy Phys. **03**, 101 (2020), doi:10.1007/JHEP03(2020)101.

[24] G. Colangelo, M. Hoferichter, A. Nyffeler, M. Passera and P. Stoffer, *Remarks on higher-order hadronic corrections to the muon $g-2$*, Phys. Lett. B **735**, 90 (2014), doi:10.1016/j.physletb.2014.06.012.

[25] T. Blum, N. Christ, M. Hayakawa, T. Izubuchi, L. Jin, C. Jung and C. Lehner, *Hadronic light-by-light scattering contribution to the muon anomalous magnetic moment from lattice QCD*, Phys. Rev. Lett. **124**, 132002 (2020), doi:10.1103/PhysRevLett.124.132002.

[26] F. Jegerlehner, *The anomalous magnetic moment of the muon*, Springer, Cham, Switzerland, ISBN 9783319635750 (2017), doi:10.1007/978-3-319-63577-4.

[27] B. Aubert et al., *Precise measurement of the $e^+e^- \to \pi^+\pi^-(\gamma)$ cross section with the initial state radiation method at BABAR*, Phys. Rev. Lett. **103**, 231801 (2009), doi:10.1103/PhysRevLett.103.231801.

[28] J. P. Lees, et al., *Precise measurement of the $e^+e^- \to \pi^+\pi^-(\gamma)$ cross section with the initial-state radiation method at BABAR*, Phys. Rev. D **86**, 032013 (2012), doi:10.1103/PhysRevD.86.032013.

[29] A. Anastasi et al., *Combination of KLOE $\sigma(e^+e^- \to \pi^+\pi^-\gamma(\gamma))$ measurements and determination of $a_\mu^{\pi^+\pi^-}$ in the energy range $0.10 < 0.95$ GeV^2*, J. High Energy Phys. **03**, 173 (2018), doi:10.1007/JHEP03(2018)173.

[30] R. R. Akhmetshin et al., *Update: A reanalysis of hadronic cross section measurements at CMD-2*, Phys. Lett. B **578**, 285 (2004), doi:10.1016/j.physletb.2003.10.108.

[31] V. M. Aul'chenko et al., *Measurement of the pion form factor in the range 1.04-1.38 GeV with the CMD-2 detector*, J. Exp. Theor. Phys. Lett. **82**, 743 (2005), doi:10.1134/1.2175241.

[32] R. R. Akhmetshin et al., *High-statistics measurement of the pion form factor in the ρ-meson energy range with the CMD-2 detector*, Phys. Lett. B **648**, 28 (2007), doi:10.1016/j.physletb.2007.01.073.

[33] M. Ablikim et al., *Measurement of the $\sigma(e^+e^- \to \pi^+\pi^-)$ cross section between 600 and 900 MeV using initial state radiation*, Phys. Lett. B **753**, 629 (2016), doi:10.1016/j.physletb.2015.11.043.

[34] T. Xiao, S. Dobbs, A. Tomaradze, K. K. Seth and G. Bonvicini, *Precision measurement of the hadronic contribution to the muon anomalous magnetic moment*, Phys. Rev. D **97**, 032012 (2018), doi:10.1103/PhysRevD.97.032012.

[35] M. N. Achasov et al., *Measurement of the $\sigma(e^+e^- \to \pi^+\pi^-)$ process cross section with the SND detector at the VEPP-2000 collider in the energy region $0.525 < \sqrt{s} < 0.883$ GeV*, J. High Energy Phys. **01**, 113 (2021), doi:10.1007/JHEP01(2021)113.

[36] T. Blum, *Lattice calculation of the lowest-order hadronic contribution to the muon anomalous magnetic moment*, Phys. Rev. Lett. **91**, 052001 (2003), doi:10.1103/PhysRevLett.91.052001.

[37] B. E. Lautrup, A. Peterman and E. de Rafael, *Recent developments in the comparison between theory and experiments in quantum electrodynamics*, Phys. Rep. **3**, 193 (1972), doi:10.1016/0370-1573(72)90011-7.

[38] E. de Rafael, *Hadronic contributions to the muon $g-2$ and low-energy QCD*, Phys. Lett. B **322**, 239 (1994), doi:10.1016/0370-2693(94)91114-2.

[39] S. Borsanyi et al., *Hadronic vacuum polarization contribution to the anomalous magnetic moments of leptons from first principles*, Phys. Rev. Lett. **121**, 022002 (2018), doi:10.1103/PhysRevLett.121.022002.

[40] S. Borsanyi et al., *Leading hadronic contribution to the muon magnetic moment from lattice QCD*, Nature **593**, 51 (2021), doi:10.1038/s41586-021-03418-1.

[41] D. Giusti, F. Sanfilippo and S. Simula, *Light-quark contribution to the leading hadronic vacuum polarization term of the muon $g-2$ from twisted-mass fermions*, Phys. Rev. D **98**, 114504 (2018), doi:10.1103/PhysRevD.98.114504.

[42] D. Giusti, V. Lubicz, G. Martinelli, F. Sanfilippo and S. Simula, *Electromagnetic and strong isospin-breaking corrections to the muon $g-2$ from lattice QCD+QED*, Phys. Rev. D **99**, 114502 (2019), doi:10.1103/PhysRevD.99.114502.

[43] D. Giusti and S. Simula, *Lepton anomalous magnetic moments in Lattice QCD+QED*, Proc. Sci. **363**, 104 (2019), doi:10.22323/1.363.0104.

[44] T. Blum et al., *Calculation of the hadronic vacuum polarization contribution to the muon anomalous magnetic moment*, Phys. Rev. Lett. **121**, 022003 (2018), doi:10.1103/PhysRevLett.121.022003.

[45] V. Gülpers, A. Juttner, C. Lehner and A. Portelli, *Isospin breaking corrections to the HVP at the physical point*, Proc. Sci. **334**, 134 (2018), doi:10.22323/1.334.0134.

[46] C. Lehner and A. S. Meyer, *Consistency of hadronic vacuum polarization between lattice QCD and the R ratio*, Phys. Rev. D **101**, 074515 (2020), doi:10.1103/PhysRevD.101.074515.

[47] B. Chakraborty et al., *Strong-isospin-breaking correction to the muon anomalous magnetic moment from lattice QCD at the physical point*, Phys. Rev. Lett. **120**, 152001 (2018), doi:10.1103/PhysRevLett.120.152001.

[48] C. T. H. Davies et al., *Hadronic-vacuum-polarization contribution to the muon's anomalous magnetic moment from four-flavor lattice QCD*, Phys. Rev. D **101**, 034512 (2020), doi:10.1103/PhysRevD.101.034512.

[49] A. Gérardin et al., *Leading hadronic contribution to $(g-2)_\mu$ from lattice QCD with $N_f = 2+1$ flavours of $O(a)$ improved Wilson quarks*, Phys. Rev. D **100**, 014510 (2019), doi:10.1103/PhysRevD.100.014510.

[50] E. Shintani et al., *Hadronic vacuum polarization contribution to the muon $g-2$ with $2+1$ flavor lattice QCD on a larger than (10 fm)^4 lattice at the physical point*, Phys. Rev. D **100**, 034517 (2019), doi:10.1103/PhysRevD.100.034517.

[51] C. Aubin, T. Blum, C. Tu, M. Golterman, C. Jung and S. Peris, *Light quark vacuum polarization at the physical point and contribution to the muon $g-2$*, Phys. Rev. D **101**, 014503 (2020), doi:10.1103/PhysRevD.101.014503.

[52] K. Maltman and C. E. Wolfe, *Isospin breaking in the relation between the $e^+e^- \to \pi^+\pi^-$ versions of $|F_\pi(s)|^2$ and implications for $(g-2)_\mu$*, Phys. Rev. D **73**, 013004 (2006), doi:10.1103/PhysRevD.73.013004.

[53] C. E. Wolfe and K. Maltman, *Models of isospin breaking in the pion form factor: Consequences for the determination of $\Pi_{\rho\omega}(m_\rho^2)$ and $(g-2)_\mu/2$*, Phys. Rev. D **80**, 114024 (2009), doi:10.1103/PhysRevD.80.114024.

[54] C. E. Wolfe and K. Maltman, *Consequences of the BABAR and KLOE data for the determination of model-dependent $\rho-\omega$ mixing effects in $\Pi_{\rho\omega}(m_\rho^2)$ and $(g-2)_\mu$*, Phys. Rev. D **83**, 077301 (2011), doi:10.1103/PhysRevD.83.077301.

[55] M. Davier et al., *The discrepancy between τ and e^+e^- spectral functions revisited and the consequences for the muon magnetic anomaly*, Eur. Phys. J. C **66**, 127 (2010), doi:10.1140/epjc/s10052-009-1219-4.

[56] J. A. Miranda and P. Roig, *New τ-based evaluation of the hadronic contribution to the vacuum polarization piece of the muon anomalous magnetic moment*, Phys. Rev. D **102**, 114017 (2020), doi:10.1103/PhysRevD.102.114017.

[57] R. Barate et al., *Measurement of the axial-vector τ spectral functions and determination of $\alpha(m_Z^2)$ from hadronic τ decays*, Eur. Phys. J. C **4**, 409 (1998), doi:10.1007/s100520050217.

[58] K. Ackerstaff et al., *Measurement of the strong coupling constant $\alpha(m_Z^2)$ and the vector and axial-vector spectral functions in hadronic tau decays*, Eur. Phys. J. C **7**, 571 (1999), doi:10.1007/s100529901061.

[59] S. Schael et al., *Branching ratios and spectral functions of τ decays: Final ALEPH measurements and physics implications*, Phys. Rep. **421**, 191 (2005), doi:10.1016/j.physrep.2005.06.007.

[60] M. Davier et al., *Update of the ALEPH non-strange spectral functions from hadronic τ decays*, Eur. Phys. J. C **74**, 2803 (2014), doi:10.1140/epjc/s10052-014-2803-9.

[61] M. Golterman, K. Maltman and S. Peris, *Tests of hadronic vacuum polarization fits for the muon anomalous magnetic moment*, Phys. Rev. D **88**, 114508 (2013), doi:10.1103/PhysRevD.88.114508.

[62] M. Golterman, K. Maltman and S. Peris, *New strategy for the lattice evaluation of the leading order hadronic contribution to $(g-2)_\mu$*, Phys. Rev. D **90**, 074508 (2014), doi:10.1103/PhysRevD.90.074508.

[63] M. Golterman, K. Maltman and S. Peris, *Determination of the NNLO low-energy constant C_{93}*, Phys. Rev. D **96**, 054027 (2017), doi:10.1103/PhysRevD.96.054027.

[64] J. Gasser and H. Leutwyler, *Chiral perturbation theory: Expansions in the mass of the strange quark*, Nucl. Phys. B **250**, 465 (1985), doi:10.1016/0550-3213(85)90492-4.

[65] H. W. Fearing and S. Scherer, *Extension of the chiral perturbation theory meson Lagrangian to order p^6*, Phys. Rev. D **53**, 315 (1996), doi:10.1103/PhysRevD.53.315.

[66] J. Bijnens, G. Colangelo and G. Ecker, *The mesonic chiral Lagrangian of order p^6*, J. High Energy Phys. **02**, 020 (1999), doi:10.1088/1126-6708/1999/02/020.

[67] K. Maltman, *Vector current correlator $\langle 0|T(V_\mu^3 V_\nu^8)|0\rangle$ to two loops in chiral perturbation theory*, Phys. Rev. D **53**, 2573 (1996), doi:10.1103/PhysRevD.53.2573.

[68] J. Bijnens and P. Talavera, *Pion and kaon electromagnetic form factors*, J. High Energy Phys. **03**, 046 (2002), doi:10.1088/1126-6708/2002/03/046.

[69] S. Aoki et al., *FLAG review 2019*, Eur. Phys. J. C **80**, 113 (2020), doi:10.1140/epjc/s10052-019-7354-7.

[70] R. Dashen, *Chiral $SU(3) \otimes SU(3)$ as a symmetry of the strong interactions*, Phys. Rev. **183**, 1245 (1969), doi:10.1103/PhysRev.183.1245.

[71] G. Ecker, J. Gasser, A. Pich and E. De Rafael, *The role of resonances in chiral perturbation theory*, Nucl. Phys. B **321**, 311 (1989), doi:10.1016/0550-3213(89)90346-5.

[72] J. Bijnens, N. Hermansson-Truedsson and S. Wang, *The order p^8 mesonic chiral Lagrangian*, J. High Energy Phys. **01**, 102 (2019), doi:10.1007/JHEP01(2019)102.

[73] Y.-S. Tsai, *Decay correlations of heavy leptons in $e^+ + e^- \to \ell^+ + \ell^-$*, Phys. Rev. D **13**, 771 (1976), doi:10.1103/PhysRevD.13.771.

[74] K. Maltman, *Constraints on hadronic spectral functions from continuous families of finite energy sum rules*, Phys. Lett. B **440**, 367 (1998), doi:10.1016/S0370-2693(98)01093-4.

[75] C. A. Dominguez and K. Schilcher, *Chiral sum rules and duality in QCD*, Phys. Lett. B **448**, 93 (1999), doi:10.1016/S0370-2693(99)00028-3.

[76] G. Amorós, J. Bijnens and P. Talavera, *Two-point functions at two loops in three flavour chiral perturbation theory*, Nucl. Phys. B **568**, 319 (2000), doi:10.1016/S0550-3213(99)00674-4.

[77] M. Antonelli, V. Cirigliano, A. Lusiani and E. Passemar, *Predicting the τ strange branching ratios and implications for V_{us}* J. High Energy Phys. **10**, 070 (2013), doi:10.1007/JHEP10(2013)070.

[78] Y. Amhis et al., *Averages of b-hadron, c-hadron, and τ-lepton properties as of 2018*, Eur. Phys. J. C **81**, 226 (2021), doi:10.1140/epjc/s10052-020-8156-7.

[79] D. Boito, M. Golterman, K. Maltman, S. Peris, M. V. Rodrigues and W. Schaaf, *Strong coupling from an improved τ vector isovector spectral function*, Phys. Rev. D **103**, 034028 (2021), doi:10.1103/PhysRevD.103.034028.

[80] P. A. Zyla et al., *Review of particle physics*, Prog. Theor. Exp. Phys. **08**, 083C01 (2020), doi:10.1093/ptep/ptaa104.

[81] C. T. H. Davies et al., *Determination of the quark condensate from heavy-light current-current correlators in full lattice QCD*, Phys. Rev. D **100**, 034506 (2019), doi:10.1103/PhysRevD.100.034506.

[82] B. Chakraborty et al., *Strange and charm quark contributions to the anomalous magnetic moment of the muon*, Phys. Rev. D **89**, 114501 (2014), doi:10.1103/PhysRevD.89.114501.